hydrology

MDPI

Article

Climatological Seasonal Cycle of River Discharge into the Oceans: Contributions from Major Rivers and Implications for Ocean Modeling

Moncef Boukthir * and Jihene Abdennadher

Materials and Fluids Laboratory—LR19ES03, IPEIT-University of Tunis, Tunis 1089, Tunisia; jihene.abdennadher@ipeit.rnu.tn

* Correspondence: moncef.boukthir@ipeit.rnu.tn

Abstract: This study presents a global assessment of the climatological seasonal variability of river discharge into the oceans, based on an expanded dataset comprising 958 gauging stations across 136 countries. Monthly discharges were compiled for 145 major rivers and tributaries, with a focus on improving the accuracy and spatial coverage of global freshwater flux estimates. Compared to previous datasets, this updated compilation includes a broader set of rivers, explicitly integrates tributary inflows, and quantifies both the absolute and relative seasonal amplitudes of discharge variability. The results reveal substantial differences among ocean basins. The Atlantic Ocean, although receiving the highest total runoff, shows relatively weak seasonal variability, with a coefficient of variation of CV = 12.6% due to asynchronous peak discharge from its major rivers (Amazon, Congo, Orinoco). In contrast, the Indian Ocean exhibits the most pronounced seasonal cycle (CV = 88.3%), driven by monsoonal rivers. The Pacific Ocean shows intermediate variability (CV = 62.1%), influenced by a combination of monsoon rains and snowmelt. At the river scale, Orinoco and Changjiang display high seasonal amplitudes, exceeding 89% of their mean flows, whereas more stable regimes are found in equatorial and temperate rivers like the Amazon and Saint Lawrence. In addition, the critical role of tributaries in altering discharge magnitude and seasonal variability is well established. This study provides high-resolution monthly discharge climatologies at global and basin scales, enhancing freshwater forcing in OGCMs. By improving the representation of land–ocean exchanges, it enables more accurate simulations of salinity, circulation, biogeochemical cycles, and climate-sensitive processes in coastal and open-ocean regions.

Keywords: river discharge; seasonal variability; salinity gradients; climate change; OGCMs

check for updates

Academic Editor: Tammo Steenhuis

Received: 5 May 2025
Revised: 28 May 2025
Accepted: 29 May 2025
Published: 12 June 2025

Citation: Boukthir, M.; Abdennadher, J. Climatological Seasonal Cycle of River Discharge into the Oceans: Contributions from Major Rivers and Implications for Ocean Modeling. *Hydrology* **2025**, *12*, 147. https://doi.org/10.3390/hydrology12060147

Copyright: © 2025 by the authors. Licensee MDPI, Basel, Switzerland. This article is an open access article distributed under the terms and conditions of the Creative Commons Attribution (CC BY) license (https://creativecommons.org/licenses/by/4.0/).

1. Introduction

As climate change progresses, understanding the variability in river discharge becomes increasingly relevant for predicting shifts in oceanic salinity patterns, sea-level rise, and ecosystem dynamics. Indeed, river discharge plays a crucial role in the interaction between freshwater and seawater, influencing salinity gradients, nutrient dispersion, and sediment transport in coastal environments [1]. In addition to influencing coastal dynamics, river discharge is also beneficial for fishing, as it is rich in mineral salts. The ocean exchanges freshwater with the atmosphere through a balance between evaporation (E) and precipitation (P), and with land via river discharge (R). While E and P have been widely studied [2], R has received relatively little attention despite its significance, largely due to a lack of comprehensive data. When freshwater from rivers mixes with saltwater from the

ocean, stratification can occur, where different salinity levels form layers, restricting vertical mixing. This stratification can affect nutrient cycling and reduce oxygen levels in coastal waters, leading to hypoxic conditions that impact marine ecosystems [3]. Additionally, river discharges can alter ocean currents and circulation by introducing buoyant freshwater plumes that interact with larger oceanic currents, impacting the distributions of heat, salinity, and other physical characteristics in coastal regions [4]. Although these effects may seem localized relative to the size of oceanic basins, salinity anomalies caused by river discharge can be transported far from river mouths by ocean currents [5]. Observations confirm that rivers, such as the Amazon, Congo, and St. Lawrence, affect ocean salinity over hundreds of kilometers [6]. The Amazon River, with an annual average discharge of approximately 209×10^3 $m^3 \cdot s^{-1}$ [7,8], is the largest freshwater contributor to the global ocean. Its plume can extend over more than one million km^2 in the western tropical Atlantic Ocean, substantially reducing sea-surface salinity and influencing upper-ocean stratification, circulation, and biogeochemical processes. The extent of the plume varies seasonally and is strongly modulated by wind-driven spreading, particularly during peak discharge periods in boreal spring and summer [8–10].

The contribution of continental waters has been estimated at 12×10^6 m^3/s [11], which accounts for nearly 10% of the estimated precipitation rate [12]. As the amount of salt in the ocean remains constant, neglecting this contribution in oceanic evolution simulations would lead to an increase in salinity in the top 50 m of the ocean. As a result, river discharge into the ocean significantly contributes to the determination and evolution of ocean surface density and should be considered a vital component of the climate system [13]. In recent years, climate change has profoundly altered hydrological cycles worldwide, leading to increased variability in river discharge [14]. For instance, the 2015–2016 El Niño event led to a 25% reduction in river discharge at the Óbidos station on the Amazon River, corresponding to a deficit of approximately 1100 km^3 of runoff between October 2015 and April 2016, compared to the 2000–2014 average [15]. This variability is primarily driven by shifts in precipitation patterns, including changes in the timing, intensity, and frequency of rainfall. In some regions, intensified rainfall has resulted in more frequent flooding; in others, prolonged droughts have led to reduced river flows. For instance, between 1971 and 2010, global runoff trends showed strong regional contrasts, with decreases of more than 10% per decade in parts of the Mediterranean, Central America, and southern South America, and increases exceeding 15% per decade in parts of northern Eurasia and southeast Asia [16]. Similarly, ref. [17] reported a projected 40–60% increase in severe soil-moisture droughts across southern Europe by the end of the century under high-emission scenarios. Recent studies [18,19] highlight that these shifts are particularly pronounced in tropical and high-latitude regions, where precipitation extremes are becoming more common. These hydrological changes not only affect local river systems but also have far-reaching consequences for global ocean circulation, salinity distribution, and biogeochemical cycles. For instance, the Amazon River, whose discharge is strongly influenced by tropical rainfall, exhibits pronounced seasonal fluctuations that are intensifying due to shifts in the timing and duration of the wet season. Similar trends are observed in other major river systems, such as the Mississippi River, where altered precipitation regimes are disrupting established hydrodynamic patterns. However, few ocean general circulation models (OGCMs) account for river runoff, which has a distinct and important impact on ocean dynamics [20].

Beyond the major ocean basins, river discharge plays a decisive role in shaping the hydrology of marginal and semi-enclosed seas, where the balance between evaporation, precipitation, and freshwater inflow is especially sensitive. For example, the Baltic Sea maintains its low surface salinity largely through river discharge, which also drives estuarine-like

outflows toward the North Sea and Norwegian Sea. Similarly, the Black Sea, White Sea, and Red Sea depend on freshwater input to regulate surface stratification, water mass transformation, and exchange dynamics with neighboring basins. These regional examples highlight the crucial, yet often underrepresented, role of river discharge in modulating salinity structure, circulation patterns, and climate sensitivity in marginal seas.

Although river discharge plays a fundamental role in regulating surface salinity, stratification, and regional circulation, it remains underrepresented in many OGCMs, largely due to the scarcity of long-term, reliable river discharge datasets. To address this critical gap, we compile and analyze an updated, large-scale dataset of monthly discharge climatologies from the world's major rivers, focusing on their contributions to the Atlantic, Pacific, and Indian Oceans, as well as the Mediterranean Sea. Beyond providing improved estimates of mean discharge, our study offers a detailed characterization of seasonal cycles, with particular attention to quantifying variability through statistical metrics such as the coefficient of variation and amplitude-to-mean ratios. We explicitly account for the influence of major tributaries, which are often neglected in global assessments but can substantially alter both mean fluxes and seasonal amplitudes. By refining seasonal climatologies and integrating tributary inflows, our work supports the development of more accurate boundary conditions for OGCMs and climate–ocean coupling studies. Furthermore, because river discharge not only shapes physical ocean properties but also governs the fluxes of nutrients, carbon, and sediments to coastal environments, our database and analyses provide essential tools for improving the modeling of biogeochemical cycles and ecosystem productivity under current and evolving climate conditions. Ultimately, this study aims to strengthen the integration of hydrological and oceanographic processes, promoting more realistic simulations of land–ocean interactions under both current and future climate conditions [21,22].

2. Materials and Methods

2.1. Global River Discharge Dataset

This study utilizes monthly river discharge data compiled from the UNESCO archives [23,24], originating from the International Hydrological Decade (IHD, 1965–1974). In recent decades, the dataset has grown significantly; while the earlier Volume II [23] included data from 37 countries and 144 gauging stations, the latest UNESCO release [24] covers 136 countries and over 958 stations, providing a broader global representation of riverine freshwater inputs. Many records extend through the 1980s and 1990s, and in some cases up to the early 2000s. However, we acknowledge that most of the data used reflect hydroclimatic conditions from the late 20th century rather than the most recent decade. While this may limit the dataset's ability to capture recent climate-driven discharge trends, it remains robust for evaluating the climatological seasonal cycle of river inputs based on long-term average conditions.

Our primary goal is to evaluate the climatological seasonal variability of river discharge into the global oceans, emphasizing the construction of a robust and spatially extensive dataset. To this end, river selection was based on several criteria aimed at maximizing data quality and relevance for oceanographic applications. Only rivers with at least two years of monthly discharge records were included to ensure meaningful seasonal characterization. The period of record for the reported discharge values varies substantially across gauging stations, ranging from less than one year to over 100 years, with an average duration of 19.3 years. Figure 1 presents the frequency distribution of record lengths from the UNESCO dataset. Rivers from North America and Europe generally exhibited the longest monitoring periods, reflecting better-established hydrological networks, while shorter records were retained in data-sparse regions to avoid geographical

bias. No weighting was applied based on the length of individual time series. Instead, we imposed a minimum threshold of two complete years to ensure that each river's seasonal cycle was sufficiently represented. While we recognize that longer records offer greater statistical robustness, we prioritized spatial representativeness and seasonal data quality over temporal uniformity. This approach aligns with the study's goal of characterizing the average climatological seasonal cycle of discharge across major global rivers, rather than long-term or interannual variability.

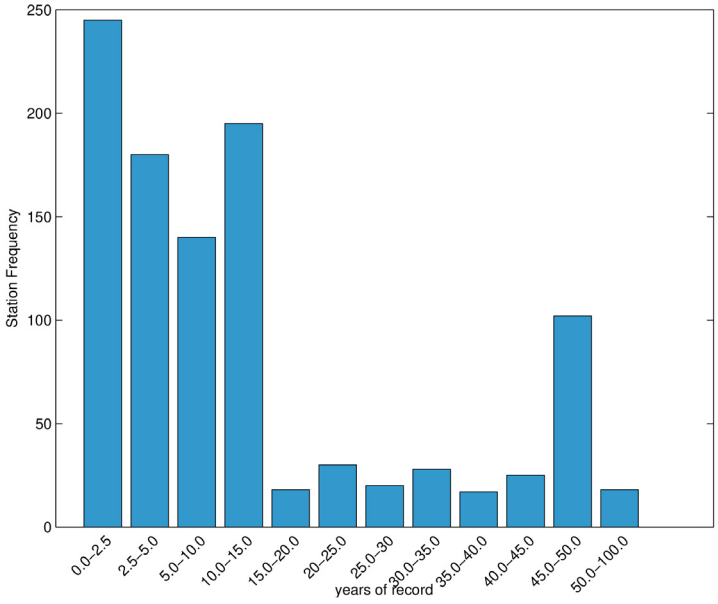

Figure 1. Frequency distribution of the record lengths (in years) for UNESCO's dataset.

To ensure that discharge estimates reflect the volume of freshwater actually reaching the ocean, we prioritized gauging stations located as close as possible to river mouths. When multiple stations were available for the same river, we used hydrological maps and global river atlases to identify and retain the most downstream station. Furthermore, in many cases, UNESCO records correspond to upstream locations, necessitating additional corrections. We incorporated downstream tributary inputs when available but only included those contributing at least 10% of the total monthly discharge for at least one month of the year. To assess the sensitivity of our results to the tributary inclusion threshold, we compared seasonal discharge estimates using both 5% and 10% thresholds for six representative rivers spanning different ocean basins. In all cases, changes in total annual discharge and seasonal amplitude were below 3%, except for the Saint Lawrence River, where the sensitivity was more pronounced. These findings confirm that our climatological results are robust with respect to this methodological choice. This threshold was selected to balance accuracy with practicality, avoiding the over-representation of numerous minor tributaries whose individual contributions are often negligible. This approach was particularly important for complex river systems, such as the Amazon and the Saint Lawrence, where tributary inflows significantly affect both the mean discharge and seasonal amplitude.

To maintain data integrity, we applied no interpolation or gap-filling to incomplete records. Stations with fragmented, inconsistent, or otherwise unreliable data were excluded. Additionally, we imposed the minimum discharge criterion that rivers must exceed 500 m^3/s for at least one month per year to be included in the final selection. This constraint ensured that only hydrologically significant rivers likely to influence coastal salinity and circulation patterns were retained. In total, we selected 145 rivers, including both primary channels and major tributaries, representing 109 distinct river mouths across the Atlantic,

Pacific, and Indian Oceans, as well as the Mediterranean Sea. Rivers from polar regions were excluded due to the predominance of cryospheric processes, such as ice cover and glacial melt, which introduce additional complexity and uncertainty in quantifying riverine freshwater fluxes [25].

2.2. Statistical Metrics

In this study, seasonal amplitude is defined as the difference between the maximum and mean discharge values. To quantify seasonal variability for each river and ocean basin, we computed the relative amplitude expressed as a percentage of the mean discharge enabling meaningful comparisons across rivers and ocean basins of varying sizes. This approach minimizes bias from absolute discharge volumes and enhances the interpretability of regional contrasts. Additionally, we calculated the coefficient of variation (CV), a dimensionless metric that represents the relative magnitude of fluctuations around the mean, defined as:

$$CV = \frac{\sigma}{\mu} \tag{1}$$

where σ is the standard deviation and μ is the mean monthly discharge. This allows for comparisons of relative seasonality across rivers of very different sizes.

To evaluate differences between this updated dataset and previous global compilations [26], we also computed the normalized root mean squared error ($NRMSE$):

$$NRMSE = \frac{RMSE}{Mean} \tag{2}$$

where $RMSE$ is the root mean square difference between discharge values from the new and reference datasets. The $NRMSE$ offers a standardized, scale-invariant error measure that supports intercomparison between river systems with differing discharge magnitudes.

Together, this methodology enables us to derive monthly discharge climatologies, evaluate their seasonal structure, and assess how different hydrological regimes (e.g., monsoonal, equatorial, snowmelt-driven) shape the timing and amplitude of freshwater inputs to the global ocean. Table 1 summarizes the hydrological regimes of the major rivers analyzed in this study, providing a useful typological context for understanding their seasonal discharge patterns.

Table 1. Hydrological regimes of major rivers.

River Name	Ocean Basin	Hydrological Regime	Characteristics
Amazon	Atlantic	Equatorial	High, year-round rainfall
Orinoco	Atlantic	Monsoonal–Equatorial	Strong summer peak linked to ITCZ migration
Ganges-Brahmaputra	Indian	Monsoonal	Strong peak in summer; low flows in winter
Mississippi	Atlantic	Mixed (Rain + Snowmelt)	Spring peak from snowmelt; moderate rainfall contribution
Changjiang	Pacific	Monsoonal	Dominated by summer monsoon rains
Congo	Atlantic	Equatorial	Wet seasons in spring and fall
St. Lawrence	Atlantic	Snowmelt-Driven	Peak in late spring; influenced by snowmelt
Nile	Mediterranean	Monsoonal-Regulated	Highly regulated

3. Results

3.1. Climatological Means

The evaluation of river discharge into the global ocean is challenged by the limited availability of long-term, high-quality, observational data, and by the scarcity of globally consistent reference datasets. To assess the reliability of our estimates, we compare our climatological annual means to two widely used datasets: the early global runoff estimate [8], which integrated numerical modeling with sparse observational data; and the river-specific discharge values compiled by [27]. In comparing to [8], we observe that while general patterns are reproduced, there are notable discrepancies in absolute values, particularly in regions with low runoff. Our discharge estimates tend to be lower than those of [8], especially outside the tropics. In contrast, better agreement is found in major tropical runoff regions, such as the western Atlantic, where observed values are more robust. This discrepancy may be explained by several methodological differences:

- the earlier study [8] relied heavily on modeling assumptions, including a quasi-steady-state global water budget, which may have resulted in overestimated discharge in arid or net-evaporative regions to preserve balance with evaporation and precipitation;
- extensive interpolation was used to fill large data gaps in [8], whereas our approach is strictly observation-based, excluding stations with fragmented or uncertain records;
- the significant increase in human water usage since the 1970s through agriculture, damming, and urbanization has reduced river discharge globally, particularly in highly developed basins [28], making comparisons to pre-1980 values potentially misleading.

To further validate our results, Table 2 presents the annual mean runoff values for major rivers in our dataset, compared to those reported by [27]. The agreement is generally strong, with most rivers showing discrepancies within ±20%, lending confidence to the updated estimates. One clear outlier is the Nile River, for which our estimate is substantially lower than the value given by [27]. This difference is likely due to methodological factors. The earlier value for the Nile may be based on pre-Aswan Dam measurements or on upstream station data, failing to account for the reduction in flow downstream due to reservoir retention, irrigation, and evaporation. Our estimate reflects post-regulation discharge, providing a more accurate representation of current riverine input to the eastern Mediterranean. Overall, these comparisons highlight the importance of using contemporary, observation-based discharge data, such as those compiled from the expanded UNESCO dataset, to accurately represent riverine contributions to the global freshwater cycle. The dataset presented here reflects the most current and comprehensive set of measurements available, allowing for improved quantification of seasonal and interannual variability in global runoff patterns.

Table 2. Annual mean river discharge (m^3/s) computed in this study (UNESCO) and by Hagemann and Dümenil (H and D, 1996), along with the differences between the two datasets.

	Rivers						
Data	Amazon	Amur	Columbia	Congo	Elbe	Godavari	Indus
UNESCO	156096	9791	5452	41129	743	3081	2647
H and D	154892	9739	5438	40250	784	3038	2244
(%) Gap	+0.8	+0.5	+0.3	+2.2	−5.2	+1.4	+18

Table 2. *Cont.*

Rivers							
Data	Mekong	Mississippi	Nile	Orinoco	Parana	Rhine	Yukon
UNESCO	8662	17701	1283	28856	17279	2287	6120
H and D	9436	14795	2926	31026	16595	2291	6347
(%) Gap	−8.2	+19.6	−56.1	−7.0	+4.1	−0.2	−3.6
Data		St. Francisco	Changjiang	St. Lawrence	Zambezi	Ganges	Nelson
UNESCO		2635	25120	7657	3342	29686	2405
H and D		2818	28936	7654	3337	33298	2403
Gap (%)		−6.5	−13.2	0	+0.1	−10.8	+0.1

3.2. Climatological Seasonal Cycles of Major Rivers

To illustrate the diversity of hydrological regimes and seasonal discharge dynamics, we analyze the climatological cycles of six major rivers: the Amazon, Congo, Orinoco, Changjiang, Mississippi, and Saint Lawrence. These rivers span a wide range of climatic zones including equatorial, monsoonal, and temperate snowmelt systems, and provide representative examples of the spatial and temporal variability in global riverine freshwater input to the ocean. Each river is characterized using indicators from Table 3, including mean discharge, seasonal amplitude, amplitude relative to the mean, and coefficient of variation (CV). Where available, the influence of tributary inflows is also assessed.

Table 3. Statistical metrics for the seasonal river discharge of five major rivers: mean, amplitude-to-mean ratio (Amp in %), standard deviation (Std), coefficient of variation (CV in %), root mean square error (RMSE), and normalized RMSE (NRMSE).

Rivers								
	Amazon	Amazon+ Tributaries	Congo	Orinoco	Changjiang	Mississippi	St. Lawrence	St. Lawrence + Tributaries
Mean	155240	163851	41117	28732	25111	17600	7654	9672
Amplitude	55298	61421	15312	30099	22556	10561	426	2916
Amp (%)	35.6	37.5	37.2	104.8	89.8	60	5.6	30.1
Std	44020	47654	7827.4	19831	13289.5	6408	440	1314.5
CV (%)	28.4	29.1	19.1	69	52.9	36.4	5.8	13.6
RMSE	2032	12557	831.4	-	589.1	2839.7	175.5	2291
NRMSE	1.3	7.7	2	2.4	2.4	16.1	2.3	24

The Amazon River, the largest freshwater contributor globally, has a mean discharge of 163851 m^3/s when tributaries are included. Its seasonal peak occurs in May–June (Figure 2), driven by intense rainfall over western Amazonia. The seasonal amplitude is 61421 m^3/s, equivalent to 37.5% of the mean, and its CV is 29.1% (Table 3), reflecting moderate month-to-month variability despite its immense volume. Excluding tributaries, as for previous assessments [29], would result in a reduction of more than 8000 m^3/s in mean discharge. These values underscore the importance of accounting for full basin contributions to accurately represent freshwater input to the tropical Atlantic Ocean.

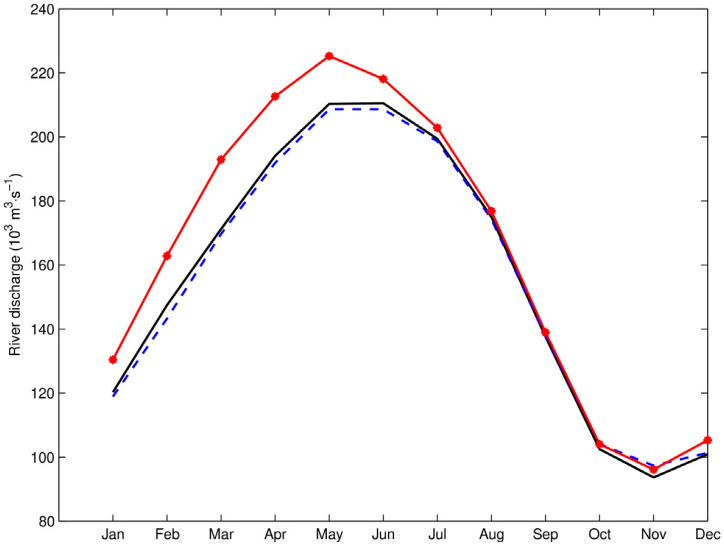

Figure 2. Climatological seasonal cycle of Amazon River discharge (10^3 m^3/s) computed in this study from UNESCO data (solid line) compared with Hagemann and Dümenil's computations (dashed line) and Amazon River discharge, including contributions from tributaries (solid line with stars).

The Congo River, second in this group, exhibits a mean discharge of 41117 m^3/s and reaches its seasonal maximum in December (Figure 3). It has a seasonal amplitude of 15312 m^3/s (37.2% of the mean) and a CV of 19.1%. Although located in the equatorial belt, the Congo shows distinct seasonal variability driven by north–south precipitation asymmetries across its vast basin. The Orinoco River typifies highly seasonal systems, with a mean discharge of 28732 m^3/s, peaks in August–September (Figure 4), roughly lagging behind the Amazon River and preceding the Congo River. Its amplitude reaches 30099 m^3/s (104.8% of the mean). Its CV is 69.1%, the highest among the rivers studied (Table 3), indicating a particularly pronounced contrast between wet and dry seasons. This variability is linked to the seasonal migration of the Intertropical Convergence Zone (ITCZ) and Venezuelan rainfall patterns. The asynchronous peak timings of the Amazon, Orinoco, and Congo contribute to a flattened composite seasonal signal in the tropical Atlantic, which weakens the seasonal salinity signal and must be represented carefully in models.

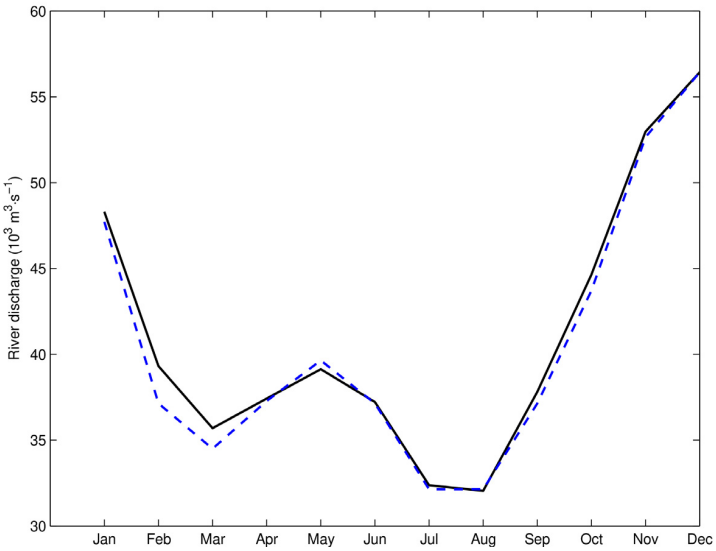

Figure 3. Climatological seasonal cycle of Congo River discharge (10^3 m^3/s) computed in this study from UNESCO data (solid line) compared with Hagemann and Dümenil's computations (dashed line).

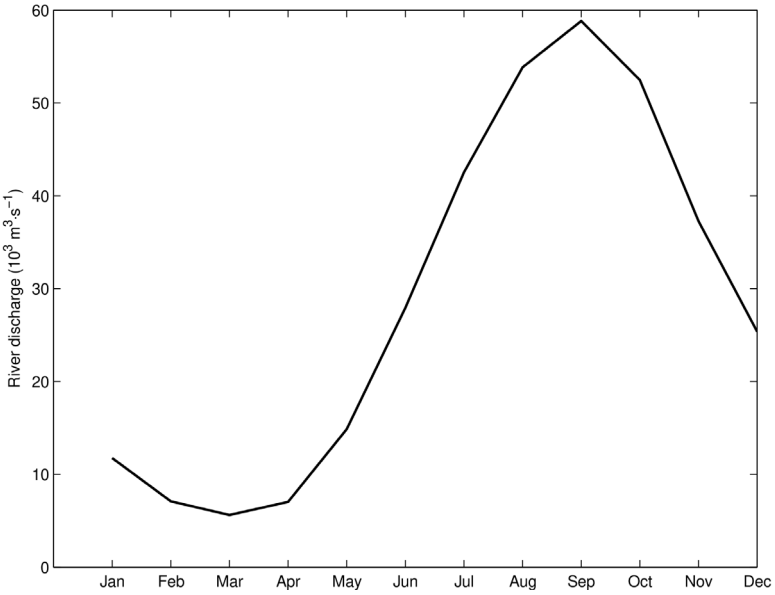

Figure 4. Climatological seasonal cycle of Orinoco River discharge (10^3 m^3/s) computed in this study from UNESCO data.

The Changjiang River, influenced by the east Asian monsoon and snowmelt from its mountainous upper basin, shows strong seasonality (Figure 5). It has a mean discharge of 25111 m^3/s, with a peak in July–August and an amplitude of 22556 m^3/s, equivalent to 89.8% of the mean (Table 3). The Changjiang, with a CV of 52.9%, exemplifies a relatively highly seasonal system, where the bulk of discharge occurs within 2–3 months. Accurate seasonal representation is therefore essential for modeling salinity anomalies, nutrient delivery, and coastal dynamics in the East China Sea. The Mississippi River, with a mean discharge of 17600 m^3/s, represents a mixed rainfall–snowmelt regime. It peaks in April–May (Figure 6), following widespread snowmelt across the U.S. Midwest. Its amplitude is 10561 m^3/s (60% of the mean). The CV is 36.4% (Table 3), reflecting a smoother seasonal cycle compared to monsoon-dominated rivers. The Mississippi remains crucial to Gulf of Mexico stratification and nutrient transport, despite its less abrupt discharge pattern. The Saint Lawrence River, including downstream tributary contributions, has a mean discharge of 9672 m^3/s. Without these tributaries, the mean would drop to 7654 m^3/s, leading to a 21% underestimation. The seasonal amplitude increases from 426 m^3/s (5.6%) to 2916 m^3/s (30.1%) when tributaries are included, while the CV rises from 5.8% to 13.6% (Table 3). The seasonal peak occurs in April–May (Figure 7), aligned with snowmelt in the Great Lakes basin. This example highlights the importance of upstream connectivity and conservative inflow accounting in representing freshwater flux in large basin–estuary systems.

Rivers, such as the Orinoco and Changjiang, which exhibit high seasonal amplitudes reaching up to 89% of the mean and a CV greater than 50% (Figure 8), illustrate the wide spectrum of seasonal variability in global river systems, ranging from highly pulsed monsoonal regimes to more stable equatorial and temperate systems. Such variability must be explicitly represented in OGCMs through seasonal runoff forcing to accurately simulate surface salinity, stratification, and biogeochemical processes in coastal and shelf environments.

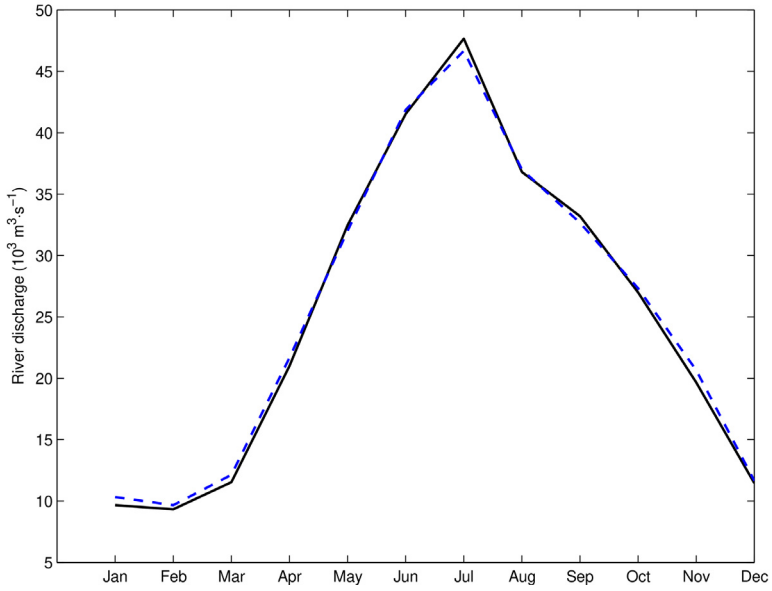

Figure 5. Climatological seasonal cycle of Changjiang River discharge (10^3 m^3/s) computed in this study from UNESCO data (solid line) compared with Hagemann and Dümenil's computations (dashed line).

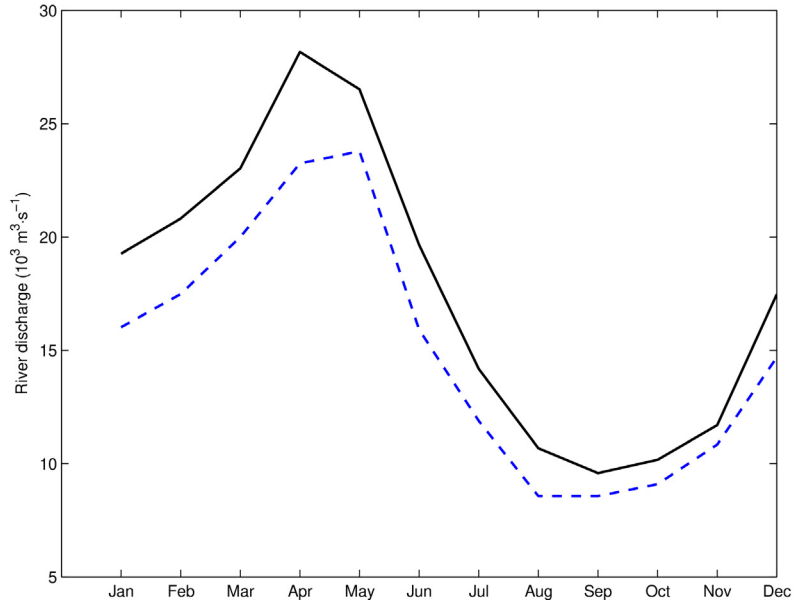

Figure 6. Climatological seasonal cycle of Mississippi River discharge (10^3 m^3/s) computed in this study from UNESCO data (solid line) compared with Hagemann and Dümenil's computations (dashed line).

3.3. Climatological Seasonal Cycles of River Discharge into the Oceans

3.3.1. Atlantic Ocean

The Atlantic Ocean receives the largest total freshwater input among all ocean basins, primarily due to the contributions of three major rivers: the Amazon, Congo, and Orinoco. These rivers dominate tropical Atlantic runoff (20° S–20° N), yet each is shaped by distinct hydroclimatic regimes, discharge magnitudes, and seasonal peak timings. The seasonal peak of the Amazon River, the world's largest in terms of discharge, occurs in May–June, following intense rainfall during the long rainy season in western Amazonia. The Orinoco River peaks in August–September, reflecting rainfall over northern South America, while the Congo River peaks in December, corresponding to wet-season precipitation over the

southern Congo Basin. These asynchronous peak timings lead to a flattened composite seasonal signal, damping the overall seasonality of freshwater input into the tropical Atlantic. This phenomenon is evident in Figure 9, which compares the combined discharge from the Amazon, Orinoco, and Congo (Rr) with the total runoff from all rivers draining into the tropical Atlantic (Ra), as reported in the UNESCO datasets [16]. Throughout the year, Ra consistently exceeds Rr, with a mean difference of 53.7 $\times$ 10^3 m^3/s, indicating that smaller and mid-sized rivers contribute significantly to the regional freshwater budget. Omitting these rivers would result in an underestimation of the total discharge by 19%. This finding aligns with prior studies [30–32], which emphasized the underestimated role of smaller river systems, particularly those draining west Africa and coastal catchments, in shaping Atlantic freshwater budgets.

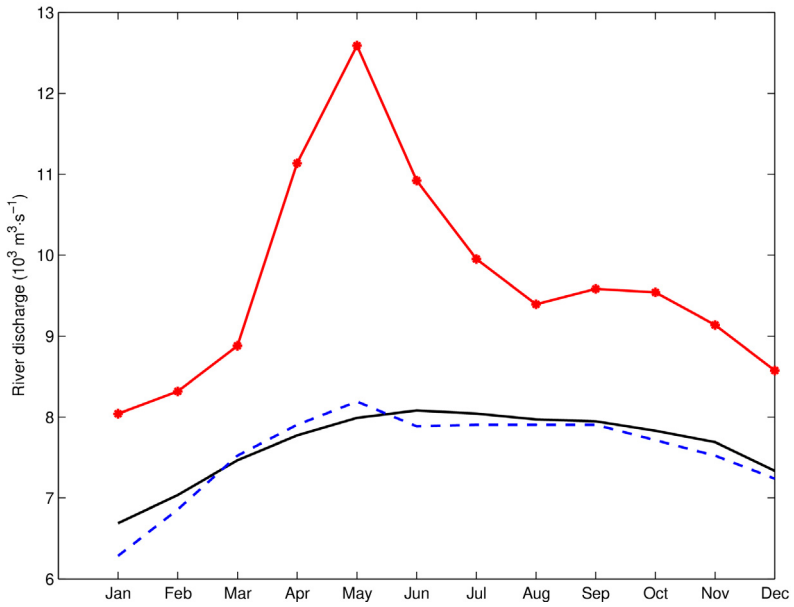

Figure 7. Climatological seasonal cycle of Saint Lawrence River discharge (10^3 m^3/s) computed in this study from UNESCO data (solid line) compared with Hagemann and Dümenil's computations (dashed line) and Saint Lawrence River discharge, including contributions from tributaries (solid line with stars).

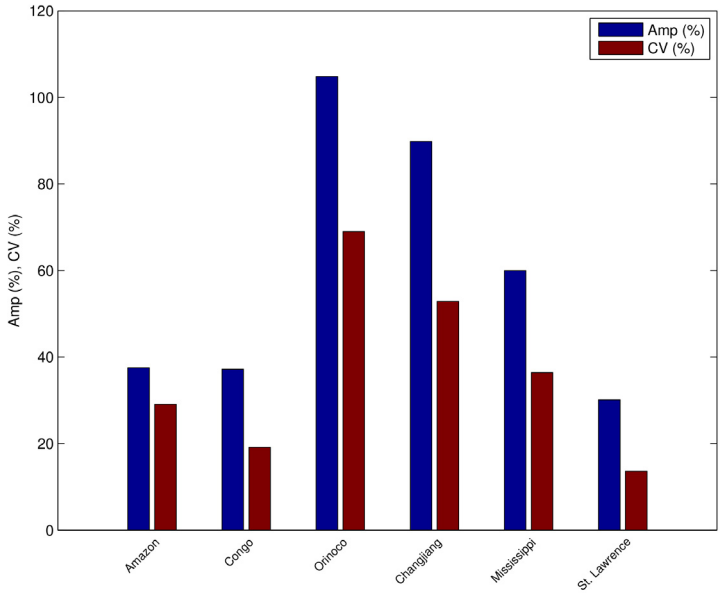

Figure 8. Histogram displaying the coefficient of variation (CV, %) and amplitude-to-mean ratio percentage (Amp, %) for the major rivers studied.

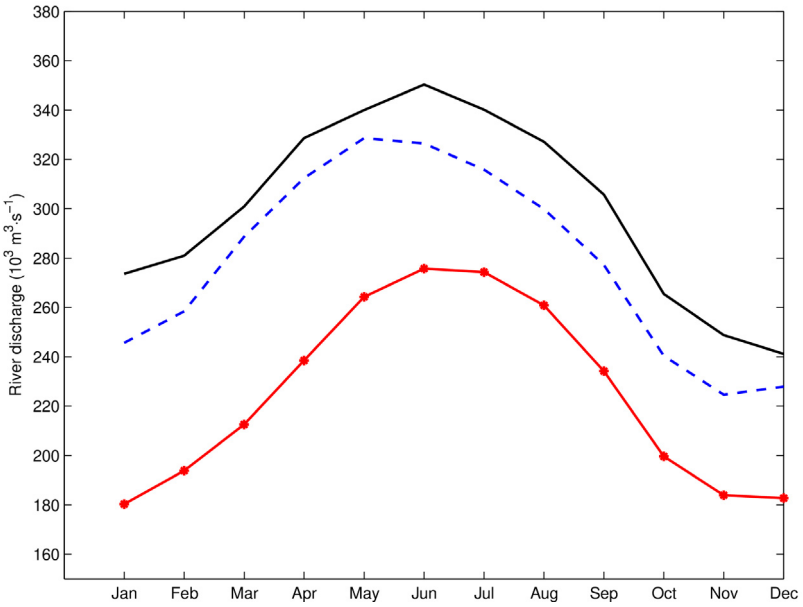

Figure 9. Climatological seasonal cycle of river discharges (in 10^3 m^3/s) from all rivers flowing into the Atlantic Ocean (solid line), the tropical Atlantic Ocean (dashed line) and, specifically, the Amazon, Congo and Orinoco rivers (solid line with stars).

The full climatological discharge cycle into the Atlantic shows a broad peak from May to July (Figure 9), reflecting the dominant influence of the Amazon, a secondary elevation in August–September due to the Orinoco, and a gradual decline into December when the Congo peaks. This multi-modal structure serves as a buffering mechanism, smoothing seasonal contrasts compared to synchronized monsoonal systems like those in the Indian Ocean. The discharge is geographically distributed across northern South America and central and west Africa, and includes smaller rivers from Equatorial Guinea, Gabon, and Ivory Coast. The diversity in rainfall regimes across these regions, ranging from equatorial year-round rainfall to northern hemisphere monsoonal systems, further flattens the aggregate seasonal cycle. Despite the high total volume, the relative seasonal variability in Atlantic freshwater input is the lowest among ocean basins (Table 4). The seasonal amplitude is 50107 m^3/s, or 16.7% of the mean discharge, and the coefficient of variation is 12.6% (Table 4). These values reflect moderate absolute variability but weak relative seasonality, largely due to phase cancellation among the major rivers. This pattern has been observed in prior studies [28,33], where the combination of distinct hydrological cycles leads to a dampened seasonal signal in freshwater input to the tropical Atlantic.

Table 4. Statistical metrics for the seasonal river discharge into the Atlantic, Pacific, and Indian Oceans, as well as the Mediterranean Sea: mean, amplitude-to-mean ratio (Amp, %), standard deviation (Std), and coefficient of variation (CV, %).

	Basins								
	Atlantic	Tropical Atlantic	Pacific	East Pacific	West Pacific	Indian	East Indian	West Indian	Mediterranean
Mean	300240	278849	66993	19732	47260	54625	41930	12695	10820
Amplitude	50107	49780	68246	30593	38343	97465	83560	13905	2790
Amp (%)	16.7	17.9	101.9	155	81.1	178.4	199.3	109.5	25.8
Std	37751	38507	41575	14291	28202	48253	42760	6170	2371
CV (%)	12.6	13.8	62.1	72.4	59.7	88.3	102	48.6	21.9

From a modeling perspective, the asynchronous discharge regime limits the development of strong seasonal salinity anomalies, particularly in the equatorial Atlantic. However, the sheer volume of freshwater, especially from the Amazon, is crucial for maintaining low surface salinity, driving upper-ocean stratification, and influencing large-scale features such as the Atlantic Meridional Overturning Circulation (AMOC). Models that neglect the timing, magnitude, or spatial distribution of this runoff risk underestimating plume dynamics, equatorial mixing, and subtropical–tropical exchanges.

3.3.2. Pacific Ocean

The Pacific Ocean receives freshwater inputs from a broad spectrum of river systems spanning high-latitude, temperate, and tropical climates. The seasonal cycle amplitude of river discharge varies significantly across its subregions, reaching approximately 114×10^3 m^3/s for the northern Pacific and just 22×10^3 m^3/s for the tropical Pacific Ocean (Figure 10). These amplitudes reflect not only the differing sizes of the contributing watersheds but also the diverse climatic regimes that govern seasonal runoff patterns. The maximum discharge occurs in June for the northern Pacific and in September for the tropical Pacific, consistent with hemispheric hydrological behavior. In the northern Pacific, spring snowmelt and intensified precipitation during late spring and early summer drive peak discharges. These patterns align with previous studies [34], which documented similar seasonal runoff trends across North America and East Asia. In the tropical Pacific, however, peak discharge is delayed, reflecting the influence of tropical rainfall systems and the onset of the summer monsoon, which typically begins later in the year [35].

Climatological annual means further highlight the hemispheric and zonal differences: the northern Pacific receives an average of 67×10^3 m^3/s, while the tropical Pacific receives only 21×10^3 m^3/s. This difference in discharge magnitude is consistent with [36], who emphasized that higher-latitude basins generally experience greater runoff due to larger catchment sizes and more intense seasonal precipitation gradients, including snowpack melt. Conversely, tropical basins, which often receive relatively uniform year-round rainfall, exhibit lower seasonal contrasts and smaller discharge amplitudes [37].

The east–west contrast within the Pacific is also pronounced. Although the seasonal cycle shape is similar between the eastern and western Pacific regions, the volume of river discharge is significantly larger on the western side of the basin (Figure 10). Specifically, the seasonal cycle amplitude is 71×10^3 m^3/s for the western Pacific, while only 43×10^3 m^3/s is recorded for the eastern Pacific. This asymmetry arises from several hydrological and climatic drivers. The western Pacific Ocean receives runoff from some of the world's largest and most hydrologically dynamic river systems, including the Mekong, Changjiang, Pearl, and Yellow rivers, whose combined catchments span diverse terrains and multiple climate zones from temperate to subtropical and monsoonal. These rivers experience substantial seasonal discharge changes, driven largely by the east and southeast Asian monsoons. The onset of the Asian monsoon triggers an intense increase in precipitation from June through August, resulting in sharp peaks in river flow during mid to late summer. In contrast, the eastern Pacific receives freshwater from North and South American rivers, such as the Columbia, Fraser, San Joaquin, and Guayas, whose catchments are often smaller and experience less intense and shorter-duration rainy seasons. The absence of large-scale monsoon systems on the eastern side of the basin limits both the magnitude and variability of runoff. Additionally, many rivers in western North America and the Andes are affected by snowmelt timing, ENSO-related variability, and drier intra-annual periods. This hemispheric and zonal heterogeneity is reflected in the Pacific Ocean's high coefficient of variation (CV = 62.1%) and large standard deviation (Table 4), indicating substantial seasonal modulation of freshwater input. The Pacific's seasonal freshwater flux is largely

governed by a combination of monsoonal rainfall in east and southeast Asia, snowmelt-driven pulses in temperate and subarctic latitudes, and interannual variability linked to regional climate phenomena such as ENSO. These findings are important for oceanographic modeling, particularly in the western Pacific, where river plumes from large systems like the Changjiang significantly affect surface salinity, stratification, and circulation patterns on the continental shelf. The discharge variability also has downstream effects on marine ecosystems, nutrient cycling, and estuarine mixing.

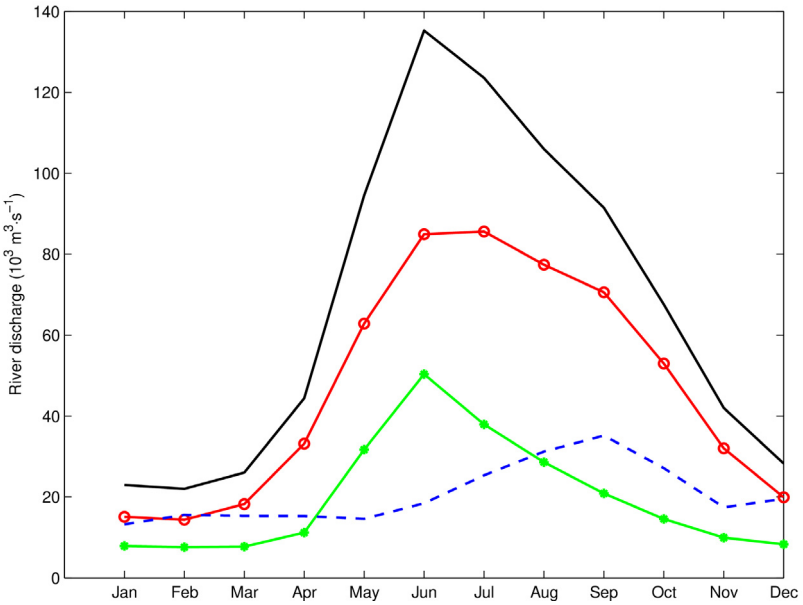

Figure 10. Climatological seasonal cycle of river discharge (10^3 m^3/s) into the northern Pacific Ocean (solid line), western Pacific Ocean (solid line with circles), eastern Pacific Ocean (solid line with stars) and tropical Pacific Ocean (dashed line).

Importantly, the seasonal amplitude of river discharge into the Pacific Ocean reaches 63.4% of the mean, ranking it among the most variable basins globally (Table 4). This high amplitude reflects the Pacific's strong sensitivity to seasonal climate drivers. Accurate discharge climatologies capturing timing and intensity are thus critical for OGCMs, particularly in monsoonal, snowmelt-dominated, and ENSO-affected regions. The Pacific exhibits sharp spatial contrasts in discharge patterns, shaped by climate, catchment size, and topography. Its seasonal variability is exceptionally high, highlighting a dynamic riverine forcing regime. These findings emphasize the need for high temporal-resolution runoff forcing in ocean–climate models to properly represent Pacific seasonal dynamics.

3.3.3. Indian Ocean

The Indian Ocean exhibits one of the most distinct and extreme seasonal cycles of river discharge among the major ocean basins, with a strong and abrupt peak driven by monsoonal rainfall. The seasonal cycle begins with low discharge values of approximately 20×10^3 m^3/s in January, rising steadily to around 25×10^3 m^3/s by May, followed by a sharp surge to a peak of 152×10^3 m^3/s in August (Figure 11). After the peak, river discharges rapidly to reach pre-monsoon levels by December. This pattern reflects the dominant influence of the Indian summer monsoon, which drives intense rainfall over large parts of the Indian subcontinent and southeast Asia from June to September. Similar discharge cycles have been reported in previous studies [38], which noted the timing and amplitude of peak river flows during the monsoon season, especially in basins such as the Ganges–Brahmaputra, Mahanadi, and Godavari.

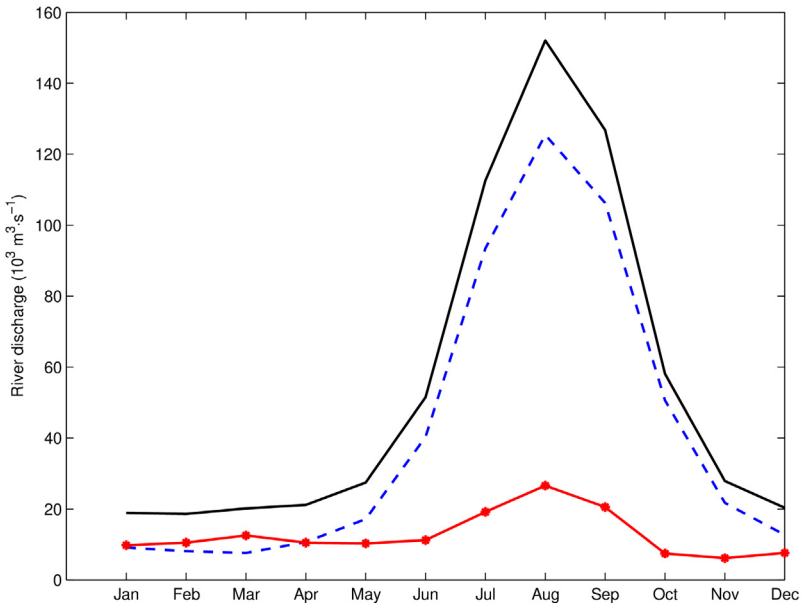

Figure 11. Climatological seasonal cycle of river discharge (10^3 m^3/s) for the entire Indian Ocean (solid line), the eastern Indian Ocean (dashed line), and the western Indian Ocean (solid line with stars).

A zonal breakdown of discharge contributions reveals stark contrasts between the eastern and western Indian Ocean. The eastern region, dominated by large river systems including the Ganges, Brahmaputra, and Irrawaddy, exhibits a peak discharge of approximately 125 $\times$ 10^3 m^3/s in August, while the western region remains far lower, not exceeding 27 $\times$ 10^3 m^3/s. Both regions follow a similar timing; however, the magnitude of the discharge from the east is more than four times greater. These results are consistent with the findings of [39], who highlighted the disproportionate influence of the eastern basin on total freshwater input to the Indian Ocean.

The Indian Ocean exhibits the most intense seasonal variability in river discharge among all ocean basins, as demonstrated by both its high coefficient of variation (CV = 88.3%) and amplitude-to-mean ratio (178.4%), as reported in Table 4 and illustrated in Figure 12. The seasonal amplitude of discharge reaches approximately 97.5 $\times$ 10^3 m^3/s, with 83.6 $\times$ 10^3 m^3/s originating from the eastern region alone. These values confirm the exceptional seasonality of the Indian Ocean's freshwater input, primarily driven by monsoonal precipitation, with minimal influence from snowmelt or glacial sources compared to the Pacific and Atlantic basins. This intense freshwater input has profound impacts on the ocean's structure and circulation. The strong seasonal pulse of discharge contributes to pronounced east–west salinity gradients, particularly in the Bay of Bengal, where significant surface freshening occurs due to river inflows, as previously documented [40–42]. The extreme seasonality of river discharge into the Indian Ocean underscores the need to account for monsoonal cycles and climate variability when assessing freshwater fluxes and their oceanographic consequences. Neglecting these inputs would result in substantial misrepresentation of regional salinity gradients, stratification, and circulation regimes in climate simulations. Our results reinforce this view, emphasizing the critical role of the timing and magnitude of river discharge in modulating upper-layer stratification, horizontal salinity contrasts, nutrient delivery, and regional ocean dynamics.

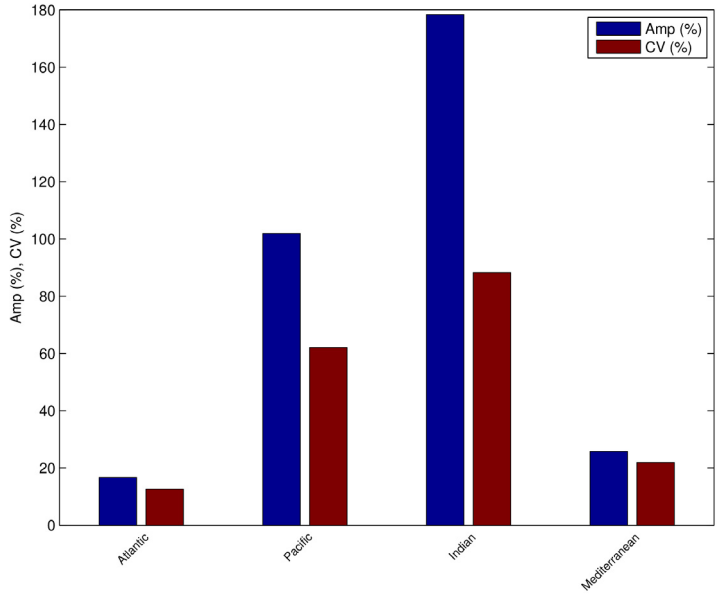

Figure 12. Histogram comparing the coefficient of variation (CV, %) and amplitude-to-mean ratio percentage (Amp, %) in river discharge across the Atlantic, Pacific, and Indian Oceans, and the Mediterranean Sea.

3.3.4. Mediterranean Sea

The seasonal variability of freshwater flux plays a central role in shaping circulation patterns in semi-enclosed basins, particularly in the Mediterranean Sea, where river discharge is one of the few key components of the surface freshwater budget [43]. In this region, the imbalance between high evaporation and relatively low precipitation and river discharge is largely compensated by the inflow of Atlantic water through the Strait of Gibraltar (G), as well as a net inflow from the Black Sea (B) via the Bosphorus. Accurately quantifying river discharge is therefore essential for understanding salinity budgets, water mass formation, and circulation variability in the Mediterranean.

The conservation of volume implies that the instantaneous flux in the Gibraltar (G) balances the flux at the air–sea interface $\int (E - P)\mathrm{dxdy}$, river discharge (R), Black Sea water inflow (B), and the accumulation of water in the basin:

$$G = \int \left(\frac{\partial \eta}{\partial t} + E - P \right) \mathrm{dxdy} - R - B \tag{3}$$

By averaging over a long period of time (10 years or more), the conservation of volume may be stated as:

$$\overline{G} = \int \left(\overline{E} - \overline{P} \right) \mathrm{dxdy} - \overline{R} - \overline{B} \tag{4}$$

A good estimate of R may lead to an accurate estimate of G, which was derived from current measurements; however, considerable scattering is observed in the proposed values [36].

The seasonal cycle of river discharge into the Mediterranean Sea exhibits a moderate amplitude of approximately 2790 m^3/s, peaking in April–May and declining toward late summer (Figure 13). The eastern basin follows a similar seasonal pattern but with a smaller amplitude of around 1415×10^3 m^3/s, reflecting the dominance of western rivers, such as the Rhone, Po, and Ebro, in total basin inflow. The climatological mean discharge estimated in this study is lower than earlier estimates reported in [44,45]; over the past two decades, dam construction, reservoir management, and irrigation have led to substantial declines in river discharge into the Mediterranean. This discrepancy is expected, given the differences

in methodology and data sources. While previous assessments relied on rainfall-derived runoff models and data from a limited number of coastal stations, our analysis is based on a larger, updated set of historical river discharge time series. These are more representative of actual observed flow; importantly, they account for recent anthropogenic impacts on river regimes. Nile River discharge has declined by nearly 50%, particularly after the construction of the Aswan High Dam [46], while the Ebro River has shown a similar reduction due to extensive water abstraction and hydraulic regulation [47]. These trends are corroborated by other studies [48] that have documented declining river flow across the Mediterranean basin as a result of intensifying human water usage, reinforcing growing concerns about regional freshwater availability and ecosystem resilience.

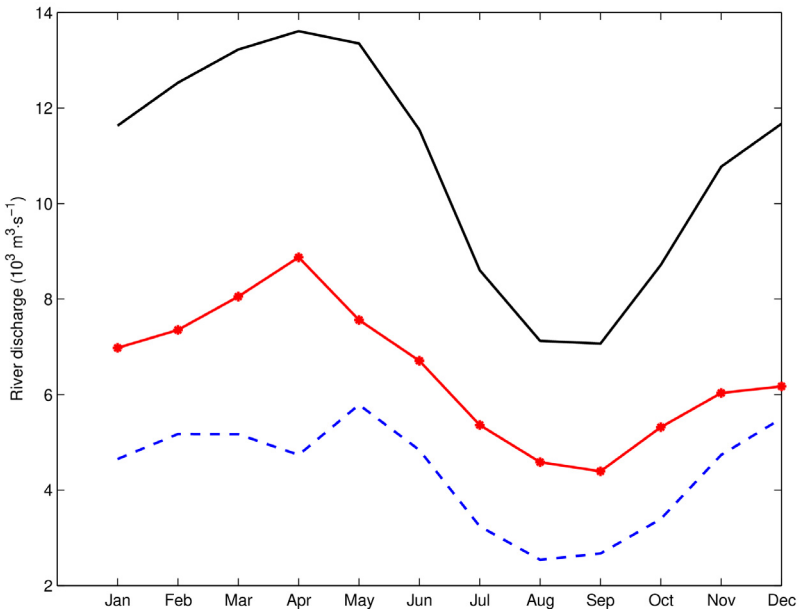

Figure 13. Climatological seasonal cycle of river discharge (in 10^3 m^3/s) for the Mediterranean Sea (solid line), as well as for its eastern basin (dashed line) and western basin (solid line with stars).

Given these considerations, we assert that our estimate of the seasonal cycle is both conservative and more accurate, as it reflects the current hydrological reality of the Mediterranean region. This view is supported by [49], who emphasized the importance of reliable river discharge data for studying hydrodynamics, biogeochemical transport, and nutrient cycling in this sensitive basin. From a variability standpoint, the coefficient of variation (CV) of river discharge into the Mediterranean is 21.9%, indicating moderate seasonal variability lower than that of the Indian (88.3%) and Pacific (62.1%) Oceans, but higher than that of the Atlantic (12.6%), as reported in Table 4 and illustrated in Figure 12. The seasonal amplitude reaches 25.8% of the mean (Table 4), confirming a significant seasonal signal in freshwater input. This variability is governed by seasonal rainfall, snowmelt from alpine catchments, and the timing of regulated water releases, all of which contribute to shaping the discharge cycle. Despite its moderate discharge levels compared to major ocean basins, the Mediterranean Sea is highly sensitive to changes in freshwater input due to its semi-enclosed configuration and limited exchange with the open ocean. Seasonal discharge fluctuations have a disproportionate effect on coastal salinity, water mass transformation, and circulation patterns, especially in marginal seas and estuarine zones. As such, even modest variations in river discharge driven by climate variability or anthropogenic stressors can alter stratification and surface-deep mixing processes, with consequences for marine ecosystems, oxygen content, and carbon cycling. Our results underscore the need for the continued monitoring of Mediterranean river discharge, and the importance of

incorporating realistic seasonal forcing into regional ocean models to improve simulations of circulation.

4. Discussion

Our analysis provides new insights into the seasonal cycles of river discharge, particularly in the Indian and Pacific Oceans, and their impact on ocean salinity gradients and circulation patterns. Although seasonal variations in river discharge may be less pronounced compared to precipitation and evaporation, their contribution to the freshwater budget is substantial and must not be overlooked [50]. Seasonal discharge cycles play a crucial role in shaping regional salinity and hydrological dynamics, especially in coastal regions where river discharge directly influences stratification, circulation, and biogeochemical processes [51].

The analysis of the main results of this study advances our understanding of continental freshwater input variability and its implications for oceanic processes, climate modeling, and hydrological-climate coupling [52]. While earlier studies offered foundational estimates of river discharge into the ocean [11,26], our work improves both spatial coverage and temporal fidelity, especially in regions that were previously underrepresented or dominated by model-derived data. Although seasonal variations in river discharge may be less pronounced compared to precipitation and evaporation, their contribution to the freshwater budget is substantial and must not be overlooked [51].

Seasonal discharge cycles play a crucial role in shaping regional salinity and hydrological dynamics, especially in coastal regions where river discharge directly influences stratification, circulation, and biogeochemical processes [53]. The seasonal variability observed across basins is strongly governed by climate regimes and basin-specific hydrological processes. Rivers in equatorial zones, such as the Congo River, show relatively stable discharge patterns due to consistent year-round precipitation. In contrast, monsoon-dominated rivers, notably the Ganges, Changjiang, and Mekong, display sharp seasonal pulses coinciding with peak rainfall events, primarily in boreal summer. Temperate and snowmelt-driven rivers, including the Mississippi and Saint Lawrence, exhibit spring maxima linked to melting snowpack and mid-latitude storm systems. These findings reinforce the importance of incorporating seasonal and climatic contexts when interpreting river discharge variability. Understanding the type of climate controlling river discharge is essential to properly assess seasonal amplitudes and their impacts on downstream salinity and circulation.

Despite being underrepresented in many OGCMs, or unused by users of these models, river discharge plays a fundamental role in shaping surface salinity, stratification, and coastal circulation. Our results show that the seasonal amplitude, expressed as a percentage of mean discharge, varies considerably from 30 to 40% in large equatorial systems, like the Amazon and Congo, to over 80% in monsoonal rivers such as the Changjiang (Table 3). At the basin scale, the Indian Ocean shows the strongest relative variability (178.4%, Table 4), driven largely by eastern rivers like the Ganges and Brahmaputra. In contrast, the Atlantic Ocean, dominated by large rivers with asynchronous peaks, exhibits a more dampened seasonal signal. These dynamics have significant implications. For instance, the eastern Indian Ocean receives a maximum river discharge of approximately 125×10^3 m^3/s in August, compared to less than 27×10^3 m^3/s in the western Indian Ocean. The corresponding climatological annual means are approximately 42×10^3 m^3/s and 13×10^3 m^3/s, respectively. This substantial disparity highlights the critical role of river discharge in establishing the east–west salinity gradient in the Indian Ocean [48], a key driver of monsoon circulation [54], with broader impacts on climate patterns across South and Southeast Asia [55].

Similarly, freshwater plumes from the Amazon, Orinoco, and Congo regulate stratification and biogeochemical cycling across the tropical Atlantic [30,32,56,57]. The Changjiang river influences nutrient supply, algal blooms, and coastal current systems in the East China Sea, while the Mississippi and Saint Lawrence Rivers significantly affect estuarine stratification and regional shelf circulation. These interactions extend beyond local ecosystems, influencing larger-scale ocean circulation and potentially contributing to global thermohaline circulation variability [58,59]. These examples illustrate the far-reaching role of river discharge not only in physical oceanography but also in ecosystem dynamics.

Given this spatial and seasonal complexity, accurate river discharge climatologies are essential for improving the freshwater boundary conditions in ocean circulation models. In particular, the differences in CV across ocean basins should guide modeling practices, especially in regions of extreme variability like the Indian Ocean. Our results strongly support this recommendation. For OGCMs to realistically simulate salinity patterns, mixed-layer dynamics, and biogeochemical processes, it is necessary to incorporate not only monthly climatologies but also realistic tributary contributions for major rivers. Our methodology explicitly addresses this point; for example, excluding tributaries from the Saint Lawrence River results in a 26% underestimation of the mean discharge and a dramatic reduction in seasonal amplitude from 30.1% to just 5.6%. Similarly, including tributaries in the Amazon increases the mean by more than 8.6×10^3 m^3/s and substantially boosts seasonal amplitude. Moreover, we observe that in some basins, the combined seasonal cycle of major rivers is muted due to asynchronous peak discharges (e.g., the Amazon, Congo, and Orinoco in the tropical Atlantic). This effect must be considered when using aggregated runoff data in models, as it affects both the magnitude and phase of seasonal freshwater delivery.

Our findings are particularly relevant in the light of recent evidence for climate-driven changes in global river flow. Anthropogenic climate forcing has been shown to contribute significantly to observed streamflow trends since the 1950s [60], while more recent analyses highlight regionally divergent runoff trends over the past five decades [61]. These include marked decreases in discharge across Mediterranean and tropical basins that are consistent with our observations of seasonal amplitude and inter-basin contrasts. Changes in precipitation patterns, increased extreme events, and expanding anthropogenic pressures, such as damming, water abstraction, and land-use change, are likely to increasingly decouple river systems from their historical discharge patterns. These evolving trends underscore the urgency of incorporating dynamic, up-to-date river discharge datasets into ocean and climate models to better represent freshwater fluxes under changing climate conditions.

As with any large-scale climatological analysis, this study has several inherent limitations. First, the duration of discharge records is heterogeneous across rivers, ranging from 2 to 178 years, with a mean duration of 19.3 years and a median of 11 years, as shown in Figure 1. While many major rivers have multi-decadal coverage, others, particularly in data-sparse regions, are represented by only a few years of observations. A minimum of two full years was required for inclusion, which ensured broader spatial coverage but may limit the capture of long-term variability in some basins. This heterogeneity in temporal coverage could introduce sampling bias, particularly for rivers subject to strong year-to-year variability. Second, although the UNESCO datasets used here are among the most comprehensive available, many discharge records terminate in the late 20th century. As a result, recent anthropogenic changes, such as increased dam construction, irrigation, and climate-driven hydrological shifts, may not be fully reflected in the dataset. Third, few gauging stations are located directly at river mouths due to tidal interference and backwater effects. To approximate actual discharge to the ocean, we used downstream summation of tributaries following established hydrological methods [62]; however, residual uncertain-

ties may persist. Despite these challenges, the updated dataset and methodology provide a robust foundation for advancing global assessments of ocean freshwater fluxes.

5. Conclusions

This study presents a comprehensive assessment of the climatological seasonal cycles of river discharge into the global ocean using an updated observational dataset derived from 958 gauging stations across 136 countries. By incorporating a broad range of river systems spanning equatorial, monsoonal, and temperate climates and explicitly accounting for downstream tributary inflows, we provide improved estimates of both mean annual discharge and seasonal variability across major ocean basins.

Our analysis reveals substantial spatial and seasonal contrasts in freshwater input. As shown in Table 3, CV values vary considerably among major rivers, from a low of 5.8% for the Saint Lawrence River, characterized by a highly regulated and stable discharge regime, to a high of 52.9% for the Changjiang River, where seasonal variability is strongly influenced by monsoonal rainfall. The Amazon River, despite its large volume, exhibits a relatively moderate CV (28.4%) due to consistent equatorial rainfall patterns, which increases slightly (29.1%) when tributary contributions are included.

At the ocean-basin scale, the Indian Ocean stands out with the highest CV (88.3%) and amplitude-to-mean ratio (178.4%), reflecting the dominance of highly seasonal rivers like the Ganges and Brahmaputra. The Pacific Ocean also exhibits significant variability (CV = 62.1%), driven by rivers such as the Changjiang and Mekong. In contrast, the Atlantic Ocean, dominated by large rivers with asynchronous seasonal peaks (e.g., Amazon, Orinoco, Congo), shows a much lower CV (12.6%). The Mediterranean Sea, while smaller in total discharge, displays a moderate CV (21.9%); its semi-enclosed nature makes it particularly sensitive to changes in river inflow. These inter-basin contrasts highlight the influence of dominant climate regimes and monsoonal, snowmelt-driven, or equatorial rainfall on runoff patterns. High seasonal variability (e.g., in the Indian Ocean) results in strong freshwater pulses that significantly impact coastal stratification, salinity gradients, nutrient delivery, and primary productivity. In contrast, basins with lower CVs sustain more constant freshwater inputs, leading to more persistent but less variable oceanographic and biogeochemical conditions. Accurately representing the timing and magnitude of freshwater forcing is thus crucial for climate and ocean models.

We emphasize the importance of incorporating relative seasonal metrics, such as the coefficient of variation and the amplitude-to-mean ratio, along with tributary contributions, to refine freshwater boundary conditions in OGCMs. Such refinements are essential to realistically simulate salinity patterns, stratification, nutrient fluxes, and regional circulation, particularly in monsoon-affected and highly seasonal regions. These insights align with recent modeling studies highlighting the sensitivity of ocean simulations to riverine input variability and the need for higher-resolution runoff forcing.

While the expanded dataset offers major improvements in spatial and temporal coverage over earlier compilations, limitations remain. These include variable record lengths, data gaps in remote or politically sensitive regions, and incomplete representation of recent anthropogenic changes (e.g., damming, abstraction). Nonetheless, the methodology and diagnostics developed here provide a robust foundation for advancing the representation of land–ocean freshwater exchanges in both climatological and dynamic modeling contexts. Overall, this study underscores the urgent need for tighter integration between hydrological and oceanographic research, particularly in the context of accelerating global change.

To support future research, we recommend integrating satellite-derived discharge estimates and other remote sensing products to enhance spatial coverage, incorporating seasonal runoff forcing into regional and global OGCMs, and prioritizing efforts to better

quantify feedback between terrestrial hydrology and oceanic processes, particularly in monsoon-affected and polar regions.

Author Contributions: Conceptualization, M.B.; methodology, M.B.; software, M.B. and J.A.; validation, J.A.; formal analysis, M.B. and J.A.; investigation, M.B.; resources, M.B.; writing—original draft preparation, M.B.; writing—review and editing, M.B. and J.A.; visualization, J.A.; supervision, M.B. All authors have read and agreed to the published version of the manuscript.

Funding: This research was funded by the Ministry of Higher Education and Scientific Research, grant number 8124-2023.

Data Availability Statement: Data are contained within the article.

Acknowledgments: The authors express their gratitude to UNESCO in Paris for granting access to the reports pertaining to the updated historical dataset.

Conflicts of Interest: The authors declare no conflicts of interest.

References

1. Mann, K.H.; Lazier, J.R.N. *Dynamics of Marine Ecosystems: Biological-Physical Interactions in the Oceans*, 3rd ed.; Wiley-Blackwell: Hoboken, NJ, USA, 2014.
2. Yu, L. Global Air–Sea Fluxes of Heat, Fresh Water, and Momentum: Energy Budget Closure and Unanswered Questions. *Annu. Rev.* **2019**, *11*, 227–248. [CrossRef] [PubMed]
3. Diaz, R.J.; Rosenberg, R. Spreading dead zones and consequences for marine ecosystems. *Science* **2008**, *321*, 926–929. [CrossRef] [PubMed]
4. Sauvage, C.; Brossier, C.L.; Ducrocq, V.; Bouin, M.N.; Vincendon, B.; Verdecchia, M.; Taupier-Letage, I.; Orain, J. Impact of the representation of the freshwater river input in the Western Mediterranean Sea. *Ocean Model.* **2018**, *131*, 115–131. [CrossRef]
5. Wang, Y.; Wu, P. Influence of riverine freshwater fluxes on global ocean salinity. *Geophys. Res. Lett.* **2017**, *44*, 7793–7801. [CrossRef]
6. Meade, R.H.; Rayol, J.M.; Conceição, A. Effect of Amazon River on the salinity of the tropical Atlantic Ocean. *J. Geophys. Res. Ocean.* **1990**, *95*, 14221–14232.
7. Masson, S.; Delecluse, P. Influence of the Amazon River on the tropical Atlantic Ocean. *Geophys. Res. Lett.* **2001**, *28*, 1981–1984. [CrossRef]
8. Dai, A.; Trenberth, K.E. Estimates of freshwater discharge from continents: Latitudinal and seasonal variations. *J. Hydrometeorol.* **2002**, *3*, 660–687. [CrossRef]
9. Coles, V.J.; Brooks, M.; Hopkins, J.; Stukel, M.R.; Yager, P.L.; Hood, R. The pathways and properties of the Amazon River Plume in the tropical North Atlantic Ocean. *J. Geophys. Res. Ocean.* **2013**, *118*, 6894–6913. [CrossRef]
10. Gévaudan, M.; Durand, F.; Jouanno, J. Amazon River discharge and the interannual variability of the Western Tropical Atlantic. *J. Geophys. Res. Ocean.* **2022**, *127*, e2022JC018495. [CrossRef]
11. Baumgartner, A.; Reichel, E. *The World Water Balance: Mean Annual Global, Continental, and Maritime Precipitation, Runoff and Evaporation*; Elsevier: Amsterdam, The Netherlands, 1975.
12. Falkowski, P.G.; Scholes, R.J.; Boyle, E.; Canadell, J.; Canfield, D.; Elser, J.; Gruber, N.; Hibbard, K.; Hogberg, P.; Linder, S.; et al. The global carbon cycle: A test of our knowledge of Earth as a system. *Science* **2008**, *290*, 291–296. [CrossRef]
13. Carmack, E.C.; Yamamoto-Kawai, M.; Haine, T.W.N.; Bacon, S.; Bluhm, B.A.; Lique, C.; Melling, H.; Polyakov, I.V.; Straneo, F.; Timmermans, M.-L.; et al. Freshwater and its role in the Arctic Marine System: Sources, disposition, storage, export, and physical and biogeochemical consequences in the Arctic and global oceans. *JGR Biogeosci.* **2015**, *121*, 675–717. [CrossRef]
14. Milly, P.C.D.; Dunne, K.A.; Vecchia, A.V. Global pattern of trends in streamflow and water availability in a changing climate. *Nature* **2005**, *438*, 347–350. [CrossRef] [PubMed]
15. van Schaik, E.; Killaars, L.; Smith, N.E.; Koren, G.; van Beek, L.P.H.; Peters, W.; van der Laan-Luijkx, I.T. Changes in surface hydrology, soil moisture and gross primary production in the Amazon during the 2015/2016 El Niño. *Philos. Trans. R. Soc. B Biol. Sci.* **2018**, *373*, 20180084. [CrossRef] [PubMed]
16. Gudmundsson, L.; Boulange, J.; Do, H.X.; Gosling, S.N.; Grillakis, M.G.; Koutroulis, A.G.; Leonard, M.; Liu, J.; Müller Schmied Papadimitriou, L.; Pokhrel, Y.; et al. Globally observed trends in mean and extreme river flow attributed to climate change. *Science* **2021**, *371*, 1159–1162. [CrossRef]
17. Grillakis, M.G. Increase in severe and extreme soil moisture droughts for Europe under climate change. *Sci. Total Environ.* **2019**, *660*, 1245–1255. [CrossRef]

18. Greve, P.; Seneviratne, S.I. Assessment of future changes in water availability and aridity. *Geophys. Res. Lett.* **2015**, *42*, 5493–5499. [CrossRef]
19. Nakhaei, P.; Ozgur, K.; Nakhaei, M.; Fathollahi-Fard, F.; Gheibi, M. Assessment of climate change on river streamflow under different representative concentration pathways. *J. Environ. Manag.* **2024**, *366*, 121754. [CrossRef]
20. Sijp, W.P.; England, M.H. The effect of river runoff on the global ocean circulation. *J. Phys. Oceanogr.* **2009**, *39*, 3024–3046.
21. Haines, K.; Valdivieso, M.; Zuo, H. Ocean salinity and the climate system. *Curr. Clim. Change Rep.* **2019**, *5*, 30–42.
22. Vörösmarty, C.J.; Green, P.; Salisbury, J.; Lammers, R.B. Global water resources: Vulnerability from climate change and population growth. *Science* **2000**, *289*, 284–288. [CrossRef]
23. UNESCO. *The United Nations World Water Development Report: Water Resources of the World*; United Nations Educational, Scientific and Cultural Organization: Paris, France, 1993; Volume II.
24. UNESCO. *Global River Discharges Database. Volume I: Africa, Volume II: Asia, and Volume III: Europe, Volume IV: North America, Volume V: South America, Volume VI: Oceania*; UNESCO: Paris, France, 1996.
25. Zhuk, V.R.; Kubryakov, A.A. Interannual Variability of the Lena River Plume Propagation in 1993–2020 during the Ice-Free Period on the Base of Satellite Salinity, Temperature, and Altimetry Measurements. *Remote Sens.* **2021**, *13*, 4252. [CrossRef]
26. Hagemann, S.; Dümenil, L. A parameterization of the lateral waterflow for the global scale. *Clim. Dyn.* **1996**, *12*, 843–856. [CrossRef]
27. UNESCO. *Studies and Reports in Hydrology, No. 1*; UNESCO: Paris, France, 1969.
28. Milliman, J.D.; Farnsworth, K.L.; Albertin, C.S. Anthropogenic influences on riverine fluxes of sediment, water, and nutrients to the coastal ocean. *BioScience* **2008**, *58*, 563–573. [CrossRef]
29. Czajkowski, J.; Maidment, D.R.; Forrest, D. A framework for aggregating high-resolution tributary inflows into global river discharge estimates. *Water Resour. Res.* **2015**, *51*, 7209–7225. [CrossRef]
30. Oltman, R.E. *Summary Report of the International Hydrological Decade (1965–1974)*; United States Geological Survey: Reston, VA, USA, 1968.
31. Meybeck, M.; Ragu, A. *River Discharges to the Oceans: An Assessment of Suspended Solids and Particulate C, N, P, and POC*; United Nations Environment Program: Nairobi, Kenya, 1996.
32. Dai, A.; Trenberth, K.E.; Qian, T. A global dataset of Palmer Drought Severity Index for 1870–2003: Relationship with soil moisture and effects of surface warming. *J. Hydrometeorol.* **2004**, *5*, 1117–1130. [CrossRef]
33. Yoo, J.; Carton, J.A. Tropical Atlantic variability and its relation to freshwater discharge from major rivers. *J. Geophys. Res. Ocean.* **1990**, *95*, 20519–20528.
34. Smith, L.C.; Pavelsky, T.M.; Shiklomanov, A.I. Hydrology of the Arctic Ocean. In *The Global Coastal Ocean*; Robinson, A.R., McCarthy, J.J., Rothschild, B.J., Eds.; Harvard University Press: Cambridge, MA, USA, 2010; pp. 679–732.
35. Jones, C.; Baker, M.L. Hydrological extremes and their impacts on climate variability. *Nat. Clim. Change* **2012**, *2*, 563–571. [CrossRef]
36. Garcia, N.O.; Mechoso, C.R.; Jones, P.D. Climatology of South Pacific River discharge. *Int. J. Climatol.* **2015**, *35*, 2671–2683. [CrossRef]
37. Brown, J.L.; Allen, M.R.; Smith, L.C. Tropical River discharge and its influence on ocean circulation and climate. *Geophys. Res. Lett.* **2017**, *44*, 6321–6330. [CrossRef]
38. Sharma, R.; Murty, V.S.N.; Suryanarayana, A. River discharge into the northern Indian Ocean and its seasonal variability. *J. Mar. Syst.* **2006**, *62*, 70–85. [CrossRef]
39. Singh, H.; Gaur, A.; Pandey, D.K. Hydrological influence of the Ganges-Brahmaputra rivers on the Indian Ocean during the monsoon season. *Geophys. Res. Lett.* **2011**, *38*, L03702.
40. Rao, S.A.; Behera, S.K.; Masumoto, Y.; Yamagata, T. A comprehensive view of the Indian Ocean during the monsoon season. *J. Oceanogr.* **2010**, *66*, 501–514.
41. Kumar, B.S.; Shankar, R. Seasonal and interannual variability of river discharge into the Indian Ocean: A global assessment. *J. Geophys. Res. Ocean.* **2014**, *119*, 2083–2102. [CrossRef]
42. Sarma, V.V.S.S.; Krishna, M.S.; Prasad, V.R.; Kumar, M.D. Salinity stratification and its influence on primary production in the Bay of Bengal. *Cont. Shelf Res.* **2013**, *66*, 63–72. [CrossRef]
43. Boukthir, M.; Barnier, B. Seasonal and interannual variations in the surface freshwater fluxes in the Mediterranean Sea. *J. Mar. Syst.* **2000**, *24*, 343–365. [CrossRef]
44. Tixeront, J. Estimation of river discharge into the Mediterranean Sea based on rainfall maps. *Ann. Géographie* **1970**, *79*, 572–576. [CrossRef]
45. Margat, J. Water resources in the Mediterranean basin. *Hydrol. Sci. J.* **1992**, *37*, 439–453. [CrossRef]
46. Wadie, W. Decreased Nile river discharge and its effects on the Mediterranean Sea. In Proceedings of the International Conference on the Nile River Basin, Cairo, Egypt, 17–19 October 2016; Volume 2, pp. 163–172.

47. Martin, J.M.; Milliman, J.D. River discharge to the Mediterranean Sea: Changes in patterns over the last century. *Glob. Planet. Change* **1997**, *14*, 75–85. [CrossRef]
48. García, C.M.; Manzano, M.; Martínez, A. Hydrological impacts of dams and irrigation on river discharge in the Mediterranean basin. *Hydrol. Process.* **2013**, *27*, 737–746. [CrossRef]
49. Dall'Olmo, G.; Lazzari, P. The role of river discharge in shaping the hydrodynamics and nutrient transport in the Mediterranean Sea. *Prog. Oceanogr.* **2014**, *120*, 52–62. [CrossRef]
50. Milliman, J.D.; Farnsworth, K.L.; Albertin, C.S. Flux and fate of fluvial sediments leaving large islands in the East Indies. *J. Geol.* **2008**, *116*, 407–428. [CrossRef]
51. Durack, P.J.; Wijffels, S.E.; Matear, R.J. Ocean salinities reveal strong global water cycle intensification during 1950 to 2000. *Science* **2012**, *336*, 455–458. [CrossRef] [PubMed]
52. Boyer, T.P.; Levitus, S.; Garcia, H.E.; Locarnini, R.A.; Stephens, C.; Antonov, J.I. Objective analyses of annual, seasonal, and monthly temperature and salinity for the world ocean on a 0.25° grid. *Int. J. Climatol.* **2005**, *25*, 931–945. [CrossRef]
53. Schott, F.A.; McCreary, J.P.; Johnson, G.C. Shallow overturning circulations of the tropical-subtropical oceans. In *Ocean Circulation and Climate: A 21st Century Perspective*; Elsevier: Amsterdam, The Netherlands, 2009; Volume 2, pp. 612–635.
54. Jensen, T.G. Modelling the seasonal undercurrent in the Somali current system. *Deep-Sea Res. Part II Top. Stud. Oceanogr.* **2001**, *48*, 1033–1069. [CrossRef]
55. Feng, M.; Zhang, N.; Liu, Q.; Wijffels, S. The Indonesian throughflow, its variability and centennial change. *Geosci. Lett.* **2018**, *5*, 3. [CrossRef]
56. Richey, J.E.; Nobre, C.A.; Deser, C. Amazon river discharge and climate variability: 1903 to 1985. *Science* **1990**, *246*, 101–103. [CrossRef]
57. Cooley, S.R.; Coles, V.J.; Subramaniam, A.; Yager, P.L. Seasonal variations in the Amazon plume-related atmospheric carbon sink. *Glob. Biogeochem. Cycles* **2009**, *21*. [CrossRef]
58. Rahmstorf, S. Ocean circulation and climate during the past 120,000 years. *Nature* **2002**, *419*, 207–214. [CrossRef]
59. Ganachaud, A.; Wunsch, C. Improved estimates of global ocean circulation, heat transport and mixing from hydrographic data. *Nature* **2000**, *408*, 453–455. [CrossRef]
60. Gudmundsson, L.; Seneviratne, S.; Zhang, X. Anthropogenic climate change detected in European renewable freshwater resources. *Nat. Clim. Change* **2017**, *7*, 813–816. [CrossRef]
61. Didovets, I.; Krysanova, V.; Nurbatsina, A.; Fallah, B.; Krylova, V.; Saparova, A.; Niyazov, J.; Kalashnikova, O.; Hattermann, F.F. Attribution of current trends in streamflow to climate change for 12 Central Asian catchments. *Clim. Change* **2024**, *177*, 16. [CrossRef]
62. Boiten, W. *Hydrometry: Measuring the Water Balance of the Catchment*, 2nd ed.; Balkema Publishers, Taylor & Francis Group: Leiden, The Netherlands, 2005; 247p.

Disclaimer/Publisher's Note: The statements, opinions and data contained in all publications are solely those of the individual author(s) and contributor(s) and not of MDPI and/or the editor(s). MDPI and/or the editor(s) disclaim responsibility for any injury to people or property resulting from any ideas, methods, instructions or products referred to in the content.